Ecosystems (2007)
DOI: 10.1007/s10021-007-9018-y

ECOSYSTEMS

Age-Dependent Changes in Ecosystem Carbon Fluxes in Managed Forests in Northern Wisconsin, USA

Asko Noormets,[1,2,*] Jiquan Chen,[1] and Thomas R. Crow[3]

[1]*Department of Earth, Ecological and Environmental Sciences, University of Toledo, 2801 W. Bancroft St., Toledo, Ohio 43606, USA;* [2]*Department of Forestry and Environmental Resources, North Carolina State University, Campus Box 7260, 920 Main Campus Dr., Raleigh, NC 27606, USA;* [3]*USDA Forest Service, WFWAR, 1601 N. kent street, Arlington, Virginia 22209, USA*

Abstract

The age-dependent variability of ecosystem carbon (C) fluxes was assessed by measuring the net ecosystem exchange of C (*NEE*) in five managed forest stands in northern Wisconsin, USA. The study sites ranged in age from 3-year-old clearcut to mature stands (65 years). All stands, except the clearcut, accumulated C over the study period from May to October 2002. Seasonal *NEE* estimates were -655 ± 17.5 g C m^{-2} in the mature hardwood (MHW), -648 ± 16.8 in the mature red pine (MRP), -195 ± 15.6 in the pine barrens (PB), $+128 \pm 17.1$ in the young hardwood clearcut (YHW), and -313 ± 14.6 in the young red pine (YRP). The age-dependent differences were similar in the hardwood and conifer forests. Even though PB was not part of either the hardwood or conifer chronosequence, and had a different disturbance agent, it still fits the same general age relationship. Higher ecosystem respiration (*ER*) in the young than in the mature stands was the combined result of earlier soil warming in spring, and higher temperature and greater biological activity in summer, as indicated by temperature-normalized respiration rates. The fire-generated PB had lower *ER* than the harvest-generated YHW and YRP, where high *ER* was sustained partly on account of logging residue. During the main growing season, the equivalent of 31 (MHW), 48 (MRP), 68 (PB), 114 (YHW) and 71% (YRP) of daily gross ecosystem production (*GEP*) was released in *ER* during the same day. The lower *ER:GEP* ratio in the mature stands was driven by greater age-dependent changes in *ER* than *GEP*. The magnitude of the increase in *ER:GEP* ratio in spring and fall was interpreted as the extent of the decoupling of *ER* and *GEP*. Decoupling (sustained high *ER* despite decreasing *GEP*) was observed in YHW, PB and MHW, whereas in coniferous stands (MRP and YRP) the stable *ER:GEP* ratio suggested preferential use of new photosynthates in *ER*. The results indicate that a great part of the variation in landscape-level C fluxes can be accounted for by mean stand age and associated parameters, which highlights the need to consider this source of heterogeneity in regional C balance estimates.

Key words: Eddy covariance; forest age; gross ecosystem production (*GEP*); managed forests; net ecosystem exchange (*NEE*); respiration; stand-replacing disturbance.

Received 4 January 2006; accepted 14 August 2006
*Corresponding author; e-mail: anoorme@ncsu.edu

Introduction

Anthropogenic and natural disturbances affect large areas of the Earth's surface (Potter and others

2003) and have significant implications for regional and global carbon (C) budgets. Disturbed forests are characterized usually by decreased short-term productivity and high respiration rates (Howard and others 2004; Humphreys and others 2005), which is the result of decreased assimilating leaf area and an increase in dead organic matter. The disturbance-induced shifts in microclimate, plant dynamics, live-to-dead biomass ratio, litter turnover and species composition have been quantified (Chen and others 1999), but their cumulative effect on regional integrated C balance is not well understood. The mosaic of young, intermediate and mature forests is likely to be spatially heterogeneous in C exchange rates (Litvak and others 2003; Chen and others 2004), but knowledge of the magnitude and functional significance of this variation is limited. Part of the uncertainty could be attributed to the confounding effects of climatic and soil gradients when comparing mature and recently disturbed stands. To minimize such effects, focused effort has been made to evaluate age-related variability in co-located stand pairs (Amiro 2001; Anthoni and others 2002).

The complexities of scaling C fluxes from stand to regional estimates are illustrated by the Chequamegon Ecosystem-Atmosphere Study, where the regionally averaging flux measurements from a very tall tower (WLEF TV tower) do not match the stand-level measurements. The measurements from WLEF show the area to be about carbon-neutral on an annual time scale (Davis and others 2003), whereas individual mixed northern hardwood stands (the predominant cover type) act as strong and consistent carbon sinks (Cook and others 2004; Desai and others 2007). Whether this is the result of high CO_2 emissions from wetlands that cover approximately 30% of the landscape (http://www.dnr.state.wi.us/maps/gis/datalandcover.html), from young recently disturbed stands, or other unaccounted factors, is still being studied. A recent modeling study by Turner and others (2003) showed that up to a fourfold difference in landscape-level net ecosystem production (*NEP*) could result from erroneous assumptions of uniform vegetation cover and ignoring heterogeneity related to post-harvest regeneration. It is not easy to quantify the broader significance of the spatial heterogeneity, but it may well be a factor contributing to the uncertainties of global C balance estimates (Houghton and others 2001).

The goal of this study was to quantify the developmental changes in C fluxes following stand-replacing disturbance. We looked for common factors that might explain the observed variability among the five closely spaced, but diverse, forest ecosystems that represent a disturbed, actively managed and climatically homogeneous forest landscape. We hypothesized that the net ecosystem exchange of C (NEE) would increase with age after a stand-replacing disturbance, driven by greater changes in gross ecosystem productivity (GEP) than in respiration (ER). We expected GEP to respond to developmental changes in the canopy leaf area index (LAI) and stand structural complexity, whereas ER would remain relatively constant and, in the absence of major changes in C input, be driven primarily by existing soil C and soil temperature.

Materials and Methods

Study area

This study was conducted in the Washburn Ranger District in the Chequamegon National Forest in northern Wisconsin, USA (46°30′–46°45′N, 91°2′–91°22′W), which belongs to the northern coniferous–deciduous biome. The topography is generally flat, with slopes less than 10° and an elevation ranging from 232 to 459 m above sea level. The soils are loamy tills with ground moraine, noncalcareous sandy loamy tills, and outwash sand (Great Lakes Ecological Assessment 2002, http://www.ncrs.fs.fed.us/gla/), with average C content in the top 10 cm 2–2.7% and N content 0.1%. The climate is humid-continental with 30-year temperature normals from −16°C in January to 25°C in July, and annual precipitation over the same period ranged from 660 to 910 mm.

The dominant vegetation types are second-growth hardwood and conifer stands, including aspen-birch (*Populus grandidentata, P. tremuloides, Betula papyrifera*), mixed northern hardwoods with sugar maple (*Acer saccharum*), red maple (*A. rubrum*) and northern red oak (*Quercus rubra*), and mixtures of white, red, and jack pine (*Pinus strobus, P. resinosa,* and *P. banksiana*). In 2001, 45% of the study landscape was covered by northern hardwood stands of different ages, 25% by red pine plantations, and 17% by pine barrens (Bresee and others 2004). Five forest stands (mature hardwood (MHW), mature red pine (MRP), pine barrens (PB), young hardwood clearcut (YHW) and young red pine (YRP)) were chosen for the current study. Of these, MHW represents a typical naturally regenerated second-growth forest in the Great Lakes Region that has been free of anthropogenic disturbance for about 70 years. MRP was planted in 1939 and has been thinned once, from 1992 to

1994. YHW and YRP represent recently clearcut stands of the same vegetation types, and PB is a fire-managed shrubland, dominated by shrubs, sedges and forbs with the regeneration of red and jack pines being controlled by a 10 to 15-year burning cycle. The harvesting practices in the hardwood and pine stands differ in the amount of logging residue, which is greater in hardwoods (Table 1) and remains scattered uniformly over the harvested area. In pine stands, the slash is piled along the ridges or around the edges of the clearcut to facilitate the planting of new seedlings. The vegetation composition of the cover types has been covered in detail by Brosofske and others (2001).

Forest Structure

Measurements of canopy structural parameters (tree age, *LAI*, percent canopy cover, basal area, amount of coarse woody debris and canopy height) were conducted in five 0.05-ha plots in each of the stands: one at the base of the eddy covariance tower and one in each cardinal direction, 100 m from the tower (Table 1). The mean stand age at each plot was determined from 10 increment cores per plot from the dominant canopy species. *LAI* was estimated on three locations per plot with a LAI-2000 plant canopy analyzer (Li-Cor) in MHW, YHW and PB, and with hemispherical photography in MHW, MRP, YHW and YRP, using the generalized LAI-2000 algorithm in the WinScanopy image processing package (Regent Instruments, Ste-Foy, Canada). The two methods agreed within 0.1 $m^2\ m^{-2}$ in MHW and YHW, where both were used. All *LAI* data were collected before dawn and after dusk during uniform sky conditions to maximize leaf-to-sky contrast on the hemispheric images, and minimize changes in light conditions between background (above-canopy) and below-canopy readings with the LAI-2000, which is sensitive to changes in the spectral quality of light. Despite precautions taken to ensure data quality, *LAI* may have been underestimated in MRP and YRP (due to foliage clumping), and PB (where most of leaf area was contributed by sedges and small shrubs). Because of these potential errors, we believe that estimates of fractional canopy cover (%) provide a more reliable and consistent basis for among-stand comparison. Canopy cover was determined with a concave densiometer (Model C, Ben Meadows Company, Janesville, USA). Stand basal area (BA, $m^2\ ha^{-1}$) was calculated from diameter at breast height of all trees in each 0.05-ha plot. The volume (V, $m^3\ ha^{-1}$) of coarse woody debris (*CWD*), defined as fallen branches and logs with a diameter of 2.5 cm and larger, was calculated for five 100-m north–south transects per stand using line-intersect method (Harmon and others 1986).

Microclimate

The following micrometeorological parameters were measured continuously in each stand. Air temperature (°C) and relative humidity (%) were measured with HMP45AC probes (Vaisala, Helsinki, Finland) at 1–4 different elevations, depending on canopy height. In MHW and MRP, four sensors were deployed: above canopy, at 0.8 and 0.5 times canopy height and at 1.8 m above ground. In YHW and PB, where canopy height was 1–2 m, only a single above-canopy sensor was deployed at 1.8 m. In YRP, two sensors were mounted at 5 and 1.8 m. Photosynthetically active radiation (*PAR*, $\mu mol\ m^{-2}\ s^{-1}$) was measured above canopy with a LI-190SB quantum sensor (Li-Cor Inc., Lincoln, NE, USA). Net radiation (R_n, $W\ m^{-2}$) was measured above canopy with a Q7.1 net radiometer (Radiation and Energy Balance Systems (REBS), Seattle, USA). Soil temperature was measured with CS107 temperature probes (Campbell Scientific Inc. (CSI), Logan, USA) at a depth of 10 cm (T_{S10}, °C), and soil moisture with CS257 gypsum moisture blocks (CSI) at a depth of 10 cm (M_{10}, kPa). All parameters were sampled every 20 s, and the 30-min averages were stored in a CR10(X) data logger (CSI). Precipitation (P, mm) was measured with a single TE525 tipping bucket rain gauge (CSI) at a permanent weather station at the University of Wisconsin Agricultural Research Station, 8–25 km from the individual stands. The seasonal dynamics of T_{S10}, M_{10} and R_n at each site, and P for the area are shown in Figure 1.

Ecosystem Gas Exchange

The *NEE* of CO_2 was measured from May to October 2002, in each forest stand using the eddy-covariance (EC) method. The towers were situated in the middle of each stand to maximize uniform fetch in all directions (30 times the sensor height in MHW and approximately 50 times the sensor height in other stands, Table 1). Each EC system included an LI–7500 open-path infrared gas analyzer (Li-Cor), a CSAT3 3-dimensional sonic anemometer (CSI) and a CR5000 data logger (CSI). The equipment was powered by four 120–150 A h deep-cycle marine batteries, recharged by solar panels (2 × 100 W). The 30-min mean fluxes of CO_2 were computed as the covariance of vertical

Table 1. Stand Characteristics of the Five Study Forests in the Washburn Ranger District of the Chequamegon National Forest for Each of Measured Patch Types

Type	Dominant species	Age (year)	Canopy cover (%)	*LAI* (m^2 m^{-2})	Basal area (m^2 ha^{-1})	*CWD* (m^3 ha^{-1})	Canopy height (m)	Sensor height (m)	Fetch (m)	Fraction of landscape (%)
MHW	*Acer rubrum* *A. saccharum* *Betula papyrifera* *Populus grandidentata* *Quercus rubra*	65	97 ± 5	3.86 ± 0.6	33.5 ± 10.6	29.1	21	26	900	40
MRP	*Pinus resinosa* *Populus grandidentata*	63	73 ± 6	2.7 ± 0.5	26.9 ± 4.6	13.5	18	23	1200	20
PB	*Andropogon scoparius* *Comptonia peregrina* *Prunus serotina* *Salix humilis* *Vaccinium angustifolium*	12	1 ± 1.2	0.2 ± 0.17	0. 1 ± 0.1	2.0	0.5	3	400	17
YHW	*Acer rubrum* *Populus grandidentata* *P. tremuloides*	3	2 ± 1.2	0.79 ± 0.6	1.5 ± 0.9	82.1	1.5	3	150	5
YRP	*Pinus banksiana* *P. resinosa*	8	17 ± 8	0.52 ± 0.3	4.7 ± 1.0	4.3	3	6	300	5

MHW mature northern hardwood, MRP mature red pine, PB pine barrens, YHW young hardwood clearcut, YRP young red pine (Mean ± SD, n = 5).

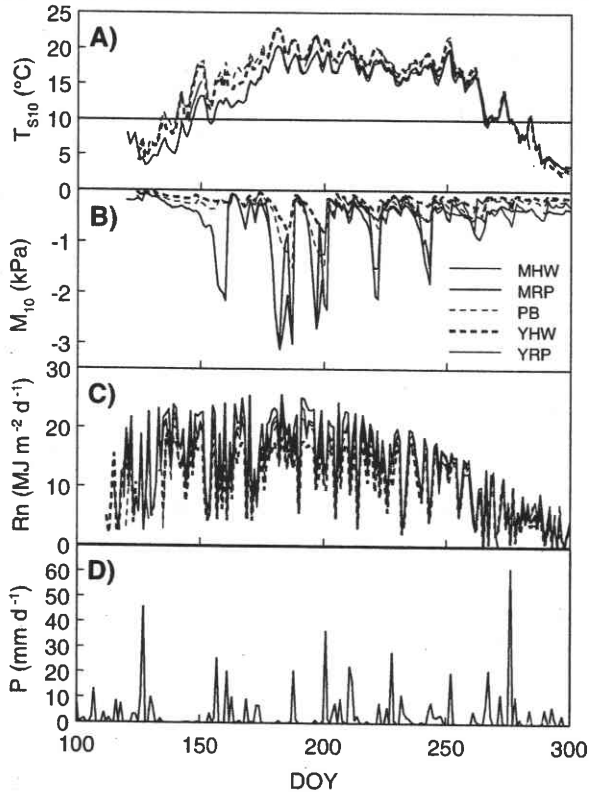

Figure 1. Annual course of daily mean soil temperature at 10 cm (**A**), soil matric potential (**B**), and daily cumulative net radiation (**C**) in five managed forest ecosystems in northern Wisconsin, USA: mature northern hardwood (MHW), mature red pine (MRP), pine barrens (PB), young hardwood clearcut (YHW) and young red pine (YRP) stands. Daily precipitation (**D**) was measured in a weather station located 8–25 km from individual study sites. To illustrate the earlier warming of soil in the young than in the mature stands, an arbitrarily chosen temperature of 10°C is marked with a *dashed line* (A).

wind speed and the concentration of CO_2, using a custom software package (EC_Processor, http://www.research.eeescience.utoledo.edu/lees/ECP/ECP.html) designed for processing open-path eddy covariance data. The algorithm uses the formulation of Leuning (2004) in the planar fit coordinate system (Wilczak and others 2001), which was defined from the entire season's mean wind data. The turbulent fluxes were adjusted for fluctuations in air density using the Webb–Pearman–Leuning expression (Webb and others 1980; Paw and others 2000). Sonic temperatures were corrected for changes in humidity and pressure (Schotanus and others 1983). The 30-min fluxes were corrected for the warming of IRGA according to Burba and others (2006).

In MHW and MRP, CO_2 storage flux in the canopy air space was estimated by measuring CO_2 concentration in the canopy air column and added to turbulent flux. Four Bev-A-Line IV tubes of equal length were used to draw air from four different heights (about 0.05×, 0.2×, 0.6× and 0.9× of canopy height) in the canopy air column. Air from all four inlets was mixed in a 5-l PVC mixing chamber prior to sampling with temperature-controlled LI-800 IRGA (Li-Cor). The flow of air (1 l min^{-1}) was regulated with a high-precision flow-meter (Model: 4112K35, McMaster-Carr, Atlanta, USA) and driven by a micro-diaphragm pump (model: NMP50, KNF Neuberger, Trenton, USA). Thus, the reported *NEE* was calculated as the sum of turbulent flux, density and IRGA heating correction terms and storage flux.

Data Integrity and Gap-filling

Data coverage from May to October was 87 (MHW), 81 (MRP), 85 (PB), 86 (YHW), and 86% (YRP). Upon screening for periods of precipitation and dew, and out-of-range values, 49–53% of data remained, and after screening for periods of low turbulence, an additional 6–12% of data were excluded from further processing, with final data coverage of 40 (MHW), 39 (MRP), 41 (PB), 45 (YHW) and 41% (YRP). Often, unusable data were identified by more than one quality control criterion. The screening protocol also excluded periods when the wind originated from behind the sensors, blowing between angles of 155° and 205° of the axis of CSAT3, although the measured fluxes exhibited no discernible directional variation. The threshold friction velocity (u^*), below which flux loss occurred (Goulden and others 1996), was determined according to Paw and others (2004), except that data were averaged by 5% bins defined by the u^* frequency distribution. The critical u^* values (u_{crit}) were 0.31 (MHW, 36% of data below u_{crit}), 0.28 (MRP, 42), 0.14 (PB, 39), 0.09 (YHW, 31) and 0.12 m s^{-1} (YRP, 38).

The median gap length was 1.5 h (3 consecutive 30-min averaging periods). Although longer gaps did occur, they were infrequent. The mean gap length was 4–5 h, and the number of gaps longer than 24 h was only 1–3 for the months of June through September, and 4–6 when including May and October, when power failures occurred. Gaps were about twice more frequent at night than during day.

Gaps in 30-min *NEE*, caused either by missing data or failure to meet the quality control criteria were filled using the rectangular hyperbola light response model with an embedded dynamic

temperature response function for ecosystem respiration (Law and others 2002):

$$NEE = R_{10} \cdot e^{\frac{Ea}{R}\left(\frac{1}{T_{ref}}-\frac{1}{T_a}\right)} + \left(\frac{\alpha \cdot \phi \cdot P_{max}}{\alpha \cdot \phi + P_{max}}\right) \quad (1)$$

where R_{10} is reference respiration, normalized to a common temperature (T_{ref} = 283.15 K = 10°C), E_a activation energy (kJ mol^{-1} K^{-1}), R universal gas constant (8.3134 J mol^{-1} K^{-1}), T_a air temperature above canopy (K), α apparent quantum yield (μmol CO_2 μmol^{-1} *PAR*), ϕ is *PAR* (μmol quanta m^{-2} s^{-1}), and P_{max} is the maximum apparent photosynthetic capacity of the canopy (μmol CO_2 m^{-2} s^{-1}). Moisture sensitivity of R_{10} was expressed as a linear function of M_{10}:

$$R_{10} = a_0 + a_1 M_{10} \quad (2)$$

where a_0 can be viewed as equivalent to R_{10} in the absence of moisture sensitivity (a_1) or at moisture saturation. Parameter a_1 indicates unit change in R_{10} per unit change in soil matric water potential (more negative M_{10} refers to drier soil). Even though the equation becomes functionally identical to Eq. 1 in the absence of moisture sensitivity, the additional parameter (a_1) affects model degrees of freedom and consequently model fit parameters. Therefore, when a_1 was not significantly different from zero, Eq. 1 was used for gapfilling purposes and the model parameter estimates and model fit parameters are reported correspondingly (Table 2). In MHW and PB, automatic model fits often failed to detect temperature sensitivity in *ER*. Therefore, an average E_a for the entire study period was used to estimate the other parameters in Eq. 1. As expected, increasing E_a from zero to a higher value led to a slight decrease in reference respiration (R_{10}), but did not have a discernible effect on the parameters of assimilatory capacity (P_{max} and α; Table 2). Typically, the amount of variation explained by these models with fixed E_a did not significantly differ from that with fitted E_a.

There was significant seasonality in both R_{10} and P_{max}, suggesting functional changes, but due to the interdependence of E_a and R_{10} (Noormets and others 2007) the significance of the changes in the former is not easy to evaluate. Throughout the study period, the parameterized models explained 69, 87, 55, 49 and 79% of the variation of *NEE* in MHW, MRP, PB, YHW and YRP, respectively (Table 2). The regression-based gapfilling method was chosen over the one based on mean diurnal variation (Falge and others 2001) because of its better performance in filling artificial gaps. We used a sign convention by which *NEE* is negative when flux is toward the surface and positive toward the atmosphere. Because respiration is positive, *GEP* was calculated as: *GEP* = *ER*–*NEE*.

Sources of Uncertainty

NEE estimates may be confounded by several sources of uncertainty and error, and may include errors in sensor calibration, spectral attenuation, u^* threshold selection, advection and gapfilling protocols. In this study, the sensors were factory calibrated at the start and end of the study. The drift at 370 ppm was −2 to + 1 ppm, which is about twice the error in factory calibration, and thus has minimal effect on the calculation of turbulent fluxes. The power spectra of three wind vectors and sonic temperature (not shown) indicated that the 10-Hz sampling frequency and 30-min averaging period for calculating the turbulent fluxes were adequate for characterizing the surface exchange at all sites. The nighttime *NEE* exhibited distinct threshold u^* and was discussed above. Below-canopy flows were not explicitly studied and advection was not quantified at any of the stands. The uncertainty in time-integrated fluxes related to gapfilling was estimated from the bias and variability of model residuals (Table 3). The residuals were averaged by month to fit the time step of model fitting, separately for day- and nighttime periods. A bias in model residuals was interpreted as systematic misrepresentation of a flux that could be corrected by adding a correction term of the same magnitude. The time-integrated fluxes (seasonal sums) were corrected for the introduced bias. The uncertainty of gapfilling was estimated as the time-integrated sum of the standard errors of monthly mean residuals, extrapolated over all gapfilled periods.

Statistical Tests

The between-site differences in micrometeorological parameters were analyzed with repeated measures analysis of variance (PROC MIXED, SAS). Differences in monthly sums of CO_2 fluxes were analyzed with simple analysis of variance (PROC ANOVA, SAS). The significance of detected differences was determined with Duncan's multiple comparison test at $P < 0.05$ level.

Results

Microclimate

The study period was approximately 1.1°C warmer than the 10-year average across the same months with slightly higher precipitation (10–80 mm),

Table 2. Parameters of Monthly Gapfilling Algorithms

Site	Month	N	Eq.	SSM	SSE	F-value	P_{max} (μmol CO_2 m^{-2} s^{-1})	(α(mol mol^{-1} m^{-2} s^{-1})	a_0, R_{10} (μmol CO_2 m^{-2} s^{-1})	a_1 (μmol CO_2 m^{-2} s^{-1} kPa^{-1} M_{10})	E_a (kJ mol^{-1} K^{-1})	R^2
MHW			1	759	1355	31	−5.72 ± 0.75	−0.0130 ± 0.0050	2.32 ± 0.34	n/a	Fit: 14798 ± 7800	0.359
	May	224	1	759	1355	41	−5.73 ± 0.76	−0.0128 ± 0.0048	2.30 ± 0.30	n/a	Fix: 15000	0.359
	Jun	898	1	84669	20624	1225	−23.3 ± 0.81	−0.0548 ± 0.0048	2.87 ± 0.28	n/a	Fit: 0 ± 0	0.804
			1	84080	21213	1182	−23.83 ± 0.90	−0.0503 ± 0.0043	2.12 ± 0.24	n/a	Fix: 15000	0.799
			1	179486	16428	3183	−31.3 ± 0.83	−0.0497 ± 0.0033	2.72 ± 0.29	n/a	Fit: 0 ± 0	0.916
	Jul	877	1	179187	16727	3121	−31.7 ± 0.88	−0.0480 ± 0.0031	1.97 ± 0.23	n/a	Fix: 15000	0.915
			1 + 2	145635	10996	2016	−30.9 ± 1.03	−0.0438 ± 0.0047	1.97 ± 0.61	0.51 ± 0.30	Fit: 0 ± 0	0.930
	Aug	613	1 + 2	145518	11113	1994	−31.1 ± 1.11	−0.0409 ± 0.0044	1.48 ± 0.55	0.40 ± 0.23	Fix: 15000	0.929
			1	145600	11059	2681	−31.0 ± 1.03	−0.0438 ± 0.0047	1.98 ± 0.61	n/a	0 ± 0	0.929
	Sep	531	1	66413	7397	1580	−23.0 ± 0.96	−0.0389 ± 0.0043	0.98 ± 0.45	n/a	Fit: 0 ± 0	0.900
			1	66389	7420	1575	−23. 2 ± 1.04	−0.0365 ± 0.0038	0.62 ± 0.35	n/a	Fix: 15000	0.899
	Oct	337	1	2046	5263	43	−6.21 ± 0.80	−0.0504 ± 0.0214	1.96 ± 0.52	n/a	Fit: 0 ± 0	0.280
			1	1942	5366	40	−5.83 ± 0.88	−0.0375 ± 0.0167	1.58 ± 0.55	n/a	Fix: 15000	0.266
MRP	May	427	1	19770	5084	411	−15.4 ± 0.72	−0.0424 ± 0.0058	1.88 ± 0.33	n/a	35491 ± 7131	0.795
	Jun	826	1	75686	17570	885	−24.3 ± 0.90	−0.0552 ± 0.0047	2.65 ± 0.34	n/a	26709 ± 5103	0.812
	Jul	848	1	113419	16052	1491	−27.66 ± 0.88	−0.0443 ± 0.0034	1.37 ± 0.28	n/a	53060 ± 7778	0.876
	Aug	632	1	133666	12825	1636	−36.9 ± 1.47	−0.0406 ± 0.0042	1.61 ± 0.52	n/a	62081 ± 12051	0.912
	Sep	452	1 + 2	88311	6369	1240	−38.7 ± 1.61	−0.0459 ± 0.0036	4.06 ± 0.70	4.06 ± 0.67	49579 ± 7386	0.933
			1	87324	7355	1329	−35.5 ± 1.52	−0.0469 ± 0.0045	1.76 ± 0.51	n/a	55110 ± 10222	0.922
	Oct	185	1	9258	1082	387	−21.5 ± 1.56	−0.0530 ± 0.0070	2.40 ± 0.47	n/a	36413 ± 10893	0.895
PB			1 + 2	388	2087	18	−1.4 ± 0.29	−0.0268 ± 0.0300	2.82 ± 0.60	7.03 ± 2.19	Fit: 27576 ± 5521	0.157
	May	481	1 + 2	382	2094	22	−1.26 ± 0.28	−0.0191 ± 0.0204	2.43 ± 0.47	6.18 ± 1.94	Fix: 34200	0.154
	Jun	874	1	339	2149	20	−1.08 ± 0.27	−0.0202 ± 0.0268	1.07 ± 0.21	n/a	29689 ± 6722	0.136
			1	11925	11502	301	−9.0 ± 0.42	−0.0469 ± 0.0080	2.89 ± 0.25	n/a	Fit: 0 ± 0	0.509
			1	10722	12704	245	−8.89 ± 0.63	−0.0261 ± 0.0043	1.07 ± 0.15	n/a	Fix: 34200	0.458
	Jul	586	1	47843	6856	1015	−19.6 ± 0.66	−0.0549 ± 0.0056	2.29 ± 0.37	n/a	Fit: 33291 ± 6091	0.875
			1	48043	6923	1353	−19.7 ± 0.64	−0.0547 ± 0.0054	2.24 ± 0.21	n/a	Fix: 34200	0.874
			1	53921	4939	1706	−22.3 ± 0.66	−0.0369 ± 0.0035	2.1 ± 0.4	n/a	Fit: 41741 ± 7106	0.916
	Aug	662	1	53913	4947	2274	−22.1 ± 0.62	−0.0389 ± 0.0032	2.49 ± 0.23	n/a	Fix: 34200	0.916
			1 + 2	14793	3738	507	−14.7 ± 0.88	−0.0200 ± 0.0030	4.07 ± 0.44	6.38 ± 1.08	Fit: 0 ± 0	0.798
	Sep	520	1 + 2	14598	3933	475	−18.7 ± 2.11	−0.0122 ± 0.0015	1.97 ± 0.26	4.08 ± 0.72	Fix: 34200	0.788
			1	14554	4405	569	−13.3 ± 0.66	−0.0258 ± 0.0042	2.54 ± 0.40	n/a	0 ± 0	0.768
			1	105	541	28	−1.56 ± 0.22	−0.0105 ± 0.0042	0.98 ± 0.12	n/a	Fit: 0 ± 0	0.163
	Oct	431	1	69	578	17	−1.53 ± 0.45	−0.0036 ± 0.0017	0.77 ± 0.12	n/a	Fix: 34200	0.107
YHW	May	497	1	1565	1476	131	−2.37 ± 0.32	−0.0101 ± 0.0042	2.36 ± 0.15	n/a	18921 ± 2990	0.515
	Jun	975	1	15942	14524	266	−10.82 ± 0.45	−0.0804 ± 0.0126	4.49 ± 0.28	n/a	7772 ± 3055	0.523
			1 + 2	33086	16181	372	−17.3 ± 0.65	−0.0715 ± 0.0076	6.72 ± 0.50	3.12 ± 0.44	17030 ± 4021	0.672
	Jul	915	1	32102	17165	426	−16.4 ± 0.63	−0.0733 ± 0.0085	5.78 ± 0.45	n/a	11543 ± 4295	0.652

Table 2. (Continued)

Site	Month	N	Eq.	SSM	SSE	F-value	P_{max} (μmol CO_2 m^{-2} s^{-1})	(α(mol mol^{-1} m^{-2} s^{-1})	a_0, R_{10} (μmol CO_2 m^{-2} s^{-1})	a_1 (μmol CO_2 m^{-2} s^{-1} kPa^{-1} M_{10})	E_a (kJ mol^{-1} K^{-1})	R^2
YRP	Aug	687	1	24745	13155	321	−17.1 ± 0.82	−0.0537 ± 0.0092	5.24 ± 0.76	n/a	13658 ± 6192	0.653
	Sep	566	1	5798	8054	101	−11.2 ± 0.77	−0.0324 ± 0.0070	3.85 ± 0.53	n/a	13824 ± 5276	0.419
	Oct	361	1	309	1477	19	−2.07 ± 0.39	−0.0262 ± 0.0164	2.02 ± 0.25	n/a	22830 ± 4324	0.173
	May	399	1	1398	1814	76	−4.39 ± 0.34	−0.0414 ± 0.0136	1.83 ± 0.28	n/a	2806 ± 4982	0.435
	Jun	829	1	30624	11593	545	−15.3 ± 0.53	−0.0655 ± 0.0071	4.74 ± 0.31	n/a	3883 ± 2987	0.725
	Jul	823	1	125753	14161	1818	−28.5 ± 0.73	−0.0600 ± 0.0044	3.88 ± 0.46	n/a	21091 ± 4835	0.899
	Aug	662	1	121095	10648	1871	−32.8 ±± 0.95	−0.0505 ± 0.0047	4.00 ± 0.65	n/a	22017 ± 6328	0.919
	Sep	586	1 + 2	52104	7375	821	−24.4 ± 0.87	−0.0473 ± 0.0050	8.63 ± 0.96	9.52 ± 1.93	4256 ± 4144	0.876
			1	51780	7734	976	−23.8 ± 0.77	−0.0545 ± 0.0038	5.03 ± 0.55	n/a	5718 ± 3943	0.870
	Oct	396	1	5526	4746	114	−7.2 ± 0.59	−0.0937 ± 0.0278	1.70 ± 0.43	n/a	5288 ± 12174	0.538

When multiple parameter sets are given, the first one is the model used for gapfilling. When E_a estimate equaled zero, the second model was fitted with E_a value forced to seasonal average (or the average of periods when it could be estimated). The last model is Eq. 1, to allow comparability across all months. Equation 1 was the preferred model for gapfilling, the combination of Eqs. 1 and 2 was used when moisture sensitivity (a_1) was significantly different from zero. All parameter estimates are given as mean ± SE. Site abbreviations listed in Table 1.

although the spring was slightly colder (0.8°C) than the long-term average (National Climatic Data Center, http://www.ncdc.noaa.gov). Mean air temperature was above freezing from 28 April through 15 October 2002. The number of frost-free days was 147 (MHW), 150 (MRP), 134 (PB), 147 (YHW) and 134 (YRP), and the number of days with T_{S10} above 10°C was 112 (MHW), 122 (MRP), 132 (PB), 138 (YHW) and 136 (YRP). Night frosts lasted throughout May and in PB three events occurred even in June. In July and August, during peak assimilation, there were only marginal differences ($P < 0.1$) between the sites in mean daily air temperature and vapor pressure deficit, with MRP, MHW and YHW having slightly higher air temperature and vapor pressure deficit than PB and YRP (data not shown). Site differences in T_{S10} and M_{10}, on the other hand, were significant ($P < 0.05$). Daily mean T_{S10} was higher in PB and YHW (19.77_A and 19.53_A°C, respectively; the subscripts indicate statistically significant difference at $P < 0.05$ as determined with ANOVA) than in MRP, MHW and YRP (17.80_B, 17.70_{BC}, and 17.48_C, respectively; Figure 1a). The open-canopy stands, YHW, YRP and PB, warmed up in spring approximately 2 weeks earlier than the mature stands, MHW and MRP (Figure 1). On average, daily mean soil matric potential was more negative in MRP (-0.97_A kPa) and MHW (-0.81_A) than in PB (-0.50_B), YRP (-0.42_B) and YHW (-0.28_B), which is likely a reflection of greater evapotranspiration in the mature stands. Net radiation also showed significant differences among sites, with the mean daily sum in July and August highest in MRP (23.85_A MJ m^{-2} day^{-1}), followed by YRP (22.38_{AB}), MHW (21.54_{AB}), PB (21.03_B) and YHW (17.69_C). In addition to higher R_n in coniferous than in hardwood stands, there was also a trend for higher R_n in mature than in the young stands, although during the period examined the age effect was significant only in hardwoods ($P < 0.05$) but not in conifers ($P = 0.19$).

Magnitude of Fluxes

The mean diurnal changes of *NEE* during different months (Figure 2) illustrate the magnitude of observed fluxes and the differences among stands during different months of the study period. The midday *NEE* was greatest in MHW, −21.5 μmol CO_2 m^{-2} s^{-1}, and slightly lower in MRP and YRP, which despite large differences in age and assimilating leaf area, exhibited a similar peak *NEE* of −16.5 and −17.4 μmol CO_2 m^{-2} s^{-1}. MRP and YRP differed, however, in the seasonal duration of CO_2

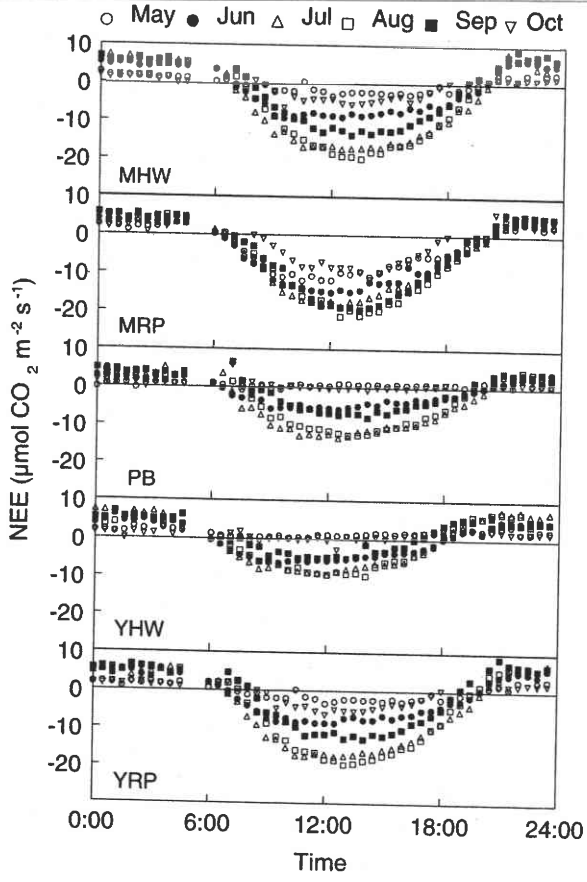

Figure 2. Monthly mean diurnal curves of measured *NEE* in five managed forest ecosystems in northern Wisconsin. *NEE* includes storage flux in MHW and MRP, whereas in the young stands, storage was assumed to be negligible (see Table 1). Because of regular dew formation on the IRGA before sunrise, the data did not meet the quality control criteria, producing gaps around 5:00–5:30 a.m. Site abbreviations listed in Figure 1.

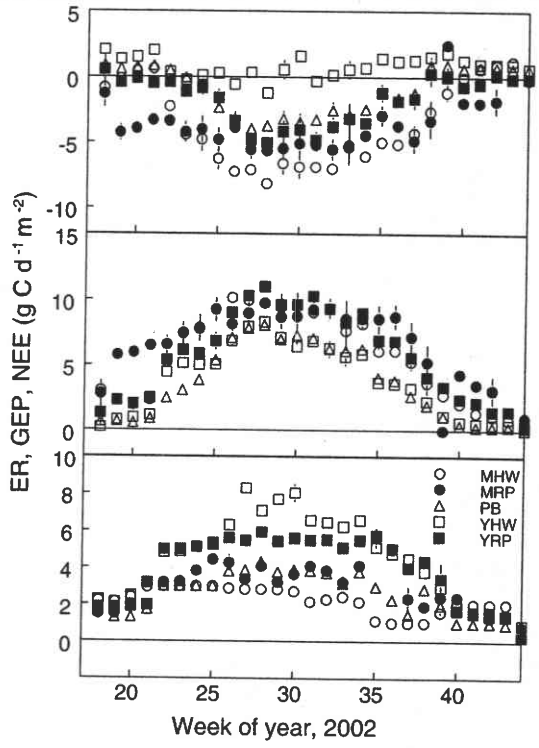

Figure 3. Seasonal course of daily *NEE* (**A**), *GEP* (**B**) and *ER* (**C**) in five managed forest ecosystems. Mean ± SE. Site abbreviations listed in Figure 1.

uptake: MRP was a consistent C sink throughout the study period, exhibiting distinctly negative *NEE* throughout May and October, whereas in YRP the magnitude of C uptake was greatly reduced during these months. PB and YHW were net sources in May and October, as was MHW, although weaker than the two young stands. The coniferous stands MRP and YRP showed greater *GEP* in May and October than the deciduous stands, but high *ER* kept daily cumulative *NEE* in YRP near C neutrality. The average nighttime *ER* (mean ± SE) in May was $2.4 \pm 0.35_A$ (MHW), $2.4 \pm 0.23_A$ (MRP), $1.0 \pm 0.24_B$ (PB), $2.5 \pm 0.2_A$ (YHW) and $1.8 \pm 0.32_{AB}$ (YRP). By July, *ER* had increased in YHW and YRP more than it had in the other stands. The average nighttime *ER* was $2.7 \pm 0.17_C$ (MHW), $3.3 \pm 0.19_C$ (MRP), $3.3 \pm 0.28_C$ (PB), $6.6 \pm 0.18_A$ (YHW), and $5.4 \pm 0.25_B$ (YRP). The duration of C uptake period was longest in MRP (162 days), followed by YRP (157), MHW (136), PB (98) and YHW (47). Upon excluding days when the daily sum was not significantly different from zero, the C uptake period decreased to 124 (MHW), 153 (MRP), 93 (PB), 15 (YHW) and 114 (YRP) days. Although the daily cumulative *GEP* was positive in all stands since early May, the equivalent of assimilated C was respired almost completely in all stands except MRP. It is noteworthy that the poorly developed canopy in YHW with large herbaceous component along with the *Populus* and *Acer* regrowth showed *GEP* comparable to mature stands. Yet, the respiratory losses that were highest in this stand resulted in net loss of C. Peak daily uptake in July (24-h *NEE*) reached −8.2 (MHW), −5.7 (MRP), −4.0 (PB), −1.2 (YHW) and −5.1 g C m^{-2} day^{-1} (YRP) (Figure 3), and cumulative *NEE* for the study period, from May to October, was -655_D (MHW), -648_D (MRP), -195_B (PB), $+128_A$ (YHW) and -313_C g C m^{-2} (YRP) (Table 3).

Gas Exchange Parameters

Equations 1 and 2 characterized an average of 67% of variability in measured *NEE* (Table 2). The fit was better during the peak growing season from

Table 3. Residuals (μmol CO_2 m^{-2} s^{-1}) of Gapfilling Models during Nighttime and Daytime Periods during Different Months (mean ± SE)

Site	Month	$R = f(T_a)$		$R = f(T_a, M)$	
		Night	Day	Night	Day
MHW	May	0.016 ± 0.389	−0.014 ± 0.182		
	Jun	−0.134 ± 0.180	0.058 ± 0.210		
	Jul	0.005 ± 0.106	−0.001 ± 0.180		
	Aug	(−0.175 ± 0.188)	(0.006 ± 0.175)	−0.081 ± 0.169	0.003 ± 0.175
	Sep	0.376 ± 0.174	−0.045 ± 0.179		
	Oct	−0.146 ± 0.328	0.029 ± 0.231		
MRP	May	0.177 ± 0.149	0.047 ± 0.215		
	Jun	−0.122 ± 0.145	0.073 ± 0.205		
	Jul	0.147 ± 0.119	0.022 ± 0.182		
	Aug	0.062 ± 0.251	0.051 ± 0.181		
	Sep	(−0.649 ± 0.220)	(−0.011 ± 0.194)	−0.738 ± 0.262	−0.018 ± 0.181
	Oct	0.239 ± 0.326	0.020 ± 0.201		
PB	May	(−0.056 ± 0.287)	(0.003 ± 0.088)	−0.056 ± 0.310	0.001 ± 0.090
	Jun	−0.103 ± 0.186	0.030 ± 0.144		
	Jul	−0.219 ± 0.275	0.042 ± 0.158		
	Aug	0.149 ± 0.215	0.004 ± 0.115		
	Sep	(0.621 ± 0.226)	(−0.051 ± 0.130)	0.847 ± 0.259	−0.070 ± 0.126
	Oct	−0.021 ± 0.107	0.005 ± 0.059		
YHW	May	−0.006 ± 0.190	0.004 ± 0.080		
	Jun	−0.103 ± 0.220	0.033 ± 0.145		
	Jul	(−0.093 ± 0.232)	(0.022 ± 0.168)	−0.058 ± 0.215	0.009 ± 0.163
	Aug	−0.545 ± 0.429	0.024 ± 0.165		
	Sep	0.370 ± 0.216	−0.046 ± 0.174		
	Oct	−0.007 ± 0.161	0.002 ± 0.129		
YRP	May	−0.042 ± 0.149	0.007 ± 0.110		
	Jun	−0.153 ± 0.220	0.037 ± 0.139		
	Jul	0.066 ± 0.160	−0.003 ± 0.161		
	Aug	0.138 ± 0.192	0.002 ± 0.160		
	Sep	(0.471 ± 0.228)	(−0.044 ± 0.162)	0.573 ± 0.258	−0.056 ± 0.158
	Oct	0.000 ± 0.139	0.000 ± 0.185		

Residuals of the moisture-inclusive model (Eqs. 1+2) are given only for months when a_1 was significantly different from zero (Table 2).

June to September, than during the transition periods in May and October, and remained higher in the coniferous than in the deciduous stands (Table 2). Model fit did not generally decrease significantly when a fixed E_a was used in MHW and PB instead of monthly fitted value, indicating that the temperature dependence of *ER* was weakly defined. The parameters of the assimilation component in Eq. 1 were insensitive to the values of R_{10} and E_a. P_{max} peaked in July and August in all stands but MRP, where the peak occurred in September. The apparent quantum yield (α) peaked in June (July in PB) and uniformly decreased through the rest of the season, marking an increase in leaf area and implying increasing environmental stress. The seasonal changes in R_{10} were more varied, with MRP, YRP and PB showing a distinct peak in September, whereas MHW and YHW exhibited a decrease. MRP, YRP and PB also exhibited significant moisture sensitivity in September, a trait not found in MHW and YHW. Temperature sensitivity (E_a) was generally lower in MHW and YHW than MRP, YRP and PB. E_a did not show clear relationship with R_{10} or a_1, but its temporal dynamics implied mutually confounding influences of moisture and temperature.

Gapfilling Uncertainty

The gapfilling model was generally unbiased, as estimated from the residuals (Table 3). The daytime residuals did not significantly differ from zero during any of the months at any site. Nighttime fluxes exhibited slightly broader variability, but were generally also not significantly different from zero. Only in September, the model underesti-

mated nighttime *NEE* at all sites, except in MRP, where the model overestimated. In addition, a systematic overestimation of nighttime *NEE* was observed in YHW in August. The variability of model residuals was generally small, smaller during daytime than nighttime, and consistent throughout the study period. Even though the error sums of squares increased with increasing magnitude of the fluxes, the variability of the residuals did not. Rather, the variability of residuals correlated with their bias (Table 3). On average, the standard error of residuals was 0.21 μmol CO_2 m^{-2} s^{-1} at night and 0.16 μmol CO_2 m^{-2} s^{-1} during day (Table 3).

Discussion

Magnitude of Fluxes

The measured *NEE* showed broad variation among the five stands. The diurnal exchange in the mature stands was of comparable magnitude to published reports from similar forests (Falge and others 2002; Schmid and others 2003; Bolstad and others 2004; Cook and others 2004). The young, recently disturbed stands YHW, YRP and PB were generally comparable to young forests of previous studies (Anthoni and others 2002; Law and others 2003; Kolari and others 2004), but the processes that occur at each site depend on climate and the nature of the disturbance, making detailed comparisons difficult. The site differences in this study were greater in *ER* than in *GEP*, and the temporal dynamics of *NEE* were strongly influenced by the dynamics of *ER*, which depended on the interactive influences of both physical and physiological parameters. For example, the soil in the young stands with low canopy cover, YHW, YRP and PB, warmed up earlier in the spring than in the mature stands. But only YHW and YRP exhibited an increase in *ER*, whereas in PB, *ER* began to increase only 4–5 weeks later (Figure 3). *ER* was similar in YHW and YRP, except in July and August, when soil temperature was 1.4–1.8°C warmer in the former. The difference between YHW and YRP on one hand, and PB on the other, correlated with the nature of the disturbance and the amount of *CWD* at the sites (Table 1). The fire-generated PB lost most of its organic matter in the burn, whereas in YHW and YRP that were created through a harvest, there is a substantial amount of logging residue that provides substrate for heterotrophic respiration. The release of unknown amounts of C during the burns certainly complicates assessing the long-term C dynamics in PB.

Errors and Uncertainties about Cumulative *NEE*

In addition to the commonly applied correction terms to turbulent fluxes (Lee and others 2004), the newly proposed correction for the warming of open-path IRGAs (Burba and others 2006) is certainly the most important one, as it addresses a major and systematic bias. Although this correction is yet to gain the broad approval of the research community, it addresses a widely recognized shortcoming in open-path eddy covariance measurements. As a result of this correction, the seasonal *NEE* increased by 27 (MHW), 8 (MRP), 29 (PB), 30 (YHW) and 34 g C m^{-2} (YRP). The term was very stable from mid-June through mid-September in terms of both seasonal and diurnal dynamics (0.14–0.16 μmol CO_2 m^{-2} s^{-1}). In early and late growing season, however, the magnitude of the term increased (0.25–0.45 μmol CO_2 m^{-2} s^{-1}) in parallel with decreasing temperatures (Burba and others 2006), and exhibited temperature-dependent diurnal cycle. Integrated over time, the correction affected *ER* about tenfold more than *GEP*.

The uncertainties introduced by gapfilling were significant during some months, and were greater during night than day. Efforts were made to correct for these. In September, when the respiration model was biased, three out of the five stands exhibited significant moisture sensitivity and it is possible that a functional change in the regulation of carbon fluxes leads to poor model performance, but the bias remained even after soil moisture was introduced to the model as an additional driving variable (Table 3). The observed biases ranged from 0.4 to 0.8 μmol CO_2 m^{-2} s^{-1}, and when extrapolated over the entire month, amounted to 5.2–10.4 g C m^{-2} $month^{-1}$. To correct for these biases, the mean bias was applied for all gapfilled periods in a given month, and the term was applied to seasonal cumulative *NEE* (Table 4). By extrapolating the standard errors of monthly mean residuals (Table 3) to all gapfilled periods, the cumulative uncertainty amounted to 14.6 to 17.5 g C m^{-2} $season^{-1}$ (Table 4).

A potential source of systematic error not considered here derives from the consistent loss of data before and during sunrise at all sites (Figure 2). Filling this 1–2 h period with modeled fluxes could, under some circumstances, result in a systematic bias (underestimating *ER*). At sites with strong respiratory sources and strong nighttime inversions, CO_2 may build up in the canopy air space in large quantities, and get washed out shortly after

Table 4. Time-integrated Carbon Fluxes (g C m^{-2}) from May to October 2002

	Age	Estimated			Corrected for gapfilling bias and uncertainty		
		NEE	*ER*	*GEP*	*NEE*	*ER*	*GEP*
MHW	65	−660	382	1042	−655 ± 17.5	387 ± 12.1	1047 ± 5.4
MRP	63	−639	523	1162	−648 ± 16.8	514 ± 12.0	1153 ± 4.8
PB	12	−205	460	663	−195 ± 15.6	470 ± 12.5	673 ± 3.1
YHW	3	+130	829	699	+128 ± 17.1	827 ± 13.3	697 ± 3.8
YRP	8	−320	732	1052	−313 ± 14.6	739 ± 10.7	1059 ± 3.9

The measured fluxes are gapfilled but not corrected for the bias of gapfilling model. The corrected fluxes include adjustments for the bias of gapfilling model (Table 3), extrapolated over all gapfilled periods. The error terms indicate uncertainty from gapfilling. The random sampling error, estimated from Richardson and others (2006) as 15–30 g C m^{-2} $season^{-1}$ applies in addition to the gapfilling uncertainty. Site abbreviations listed in Table 1.

sunrise when the convective layer re-develops. Another uncertainty about the long-term C balance, but one that does not directly affect the current study, comes from the unaccounted loss of C in fire at PB. The best estimate for the fire-mediated losses might be through biometric measurements before and after the burn, because it is difficult to capture the CO_2 spike with eddy covariance, particularly when the burn does not completely fill the flux footprint area.

The random sampling error, due to the turbulent nature of the surface-atmosphere gas exchange, is often found to be 15–25% of the observed flux (Davis and others 2003; Richardson and others 2006). Its effect on time-integrated fluxes, however, is minor because the error is not systematic. Both the above studies estimated the annual uncertainty on the order of ±20–40 g C m^2 $year^{-1}$ even though the annual *NEE* itself differed greatly between the sites. Richardson and others (2006) used day-pairs with similar meteorological conditions to estimate random sampling error at seven Ameriflux sites. They found that this error (1) increased with the magnitude of the flux, (2) was inversely proportional to wind speed, and (3) was greater for positive than negative fluxes. Although the magnitude of the error increased with the magnitude of the flux, the relative error decreased. We assume that this random sampling error of similar magnitude applies on top of the gapfilling errors in all our study sites. The combined uncertainty from the random sampling error and gapfilling error is likely 30–50 g C m^{-2} $season^{-1}$, which is less than the observed differences between individual stands (except between MHW and MRP; Table 4).

ER:*GEP* ratio

The *ER*:*GEP* ratio, which reflects an ecosystem's C sequestration potential, varied little between weeks 22 and 37 (early June through mid-September),

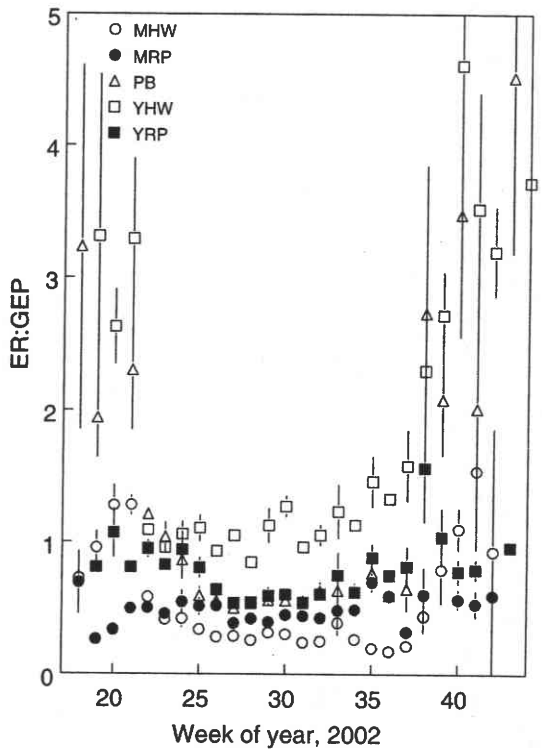

Figure 4. The weekly mean of the ratio of daily sums of *ER* and *GEP* in five managed forest ecosystems. Mean ± SE. Site abbreviations listed in Figure 1.

averaging 0.31 (MHW), 0.48 (MRP), 0.68 (PB), 1.14 (YHW) and 0.71 (YRP) (Figure 4). The values for the mature stands were slightly lower than those reported by Falge and others (2002) as growing season means for mature cold temperate forests (0.5–0.65). The greater *ER* in the young stands suggests that the decomposition of older, more recalcitrant C pools in *CWD*, litter and soil exceeded the contribution of greater living biomass in the mature stands. This is consistent with the results from 18 EuroFlux study sites, where the

annual *ER* was 49% of *GEP* in the mature non-disturbed forests, but 80% in young and recently disturbed forests (Janssens and others 2001).

The ranking of sites in terms of the *ER:GEP* ratio (YHW > YRP = PB > MRP ≥ MHW) correlates with the time since the last stand-replacing disturbance. This gradient distinguishes the stands in terms of standing biomass, canopy cover, *CWD* and microclimate. These differences reflect disturbance-induced shifts in C distribution between different pools and the contribution of these pools to *ER*. The low *ER:GEP* ratio in early and late season in MRP and YRP suggests that these two fluxes remained coupled, that is, much of the substrate for *ER* originated from newly assimilated C (Högberg and others 2001), because of the continuing assimilation in these evergreen stands. In YHW and PB (and to a lesser extent in MHW), where the *ER:GEP* ratio increased, the slower decline in *ER* than in *GEP* could be attributed to the abundance of *CWD* and litter. Although *ER* increased in spring at a similar rate and time in both YHW and YRP, the *ER:GEP* ratio suggests that the substrate for *ER* was newly assimilated C in YRP, and old, dead C (including *CWD*) in YHW.

Relations to Age and Disturbance

The differences among sites were distinct for all fluxes, with the most pronounced effects in *NEE* (Table 4). The between-site differences by far exceeded the boundaries of estimation uncertainty at any given site (except between MHW and MRP). The magnitude of the *NEE* differences was proportional to differences in age, that is, the fluxes (*NEE*, *ER* and *GEP*) differed more between MHW and YHW than between MRP and YRP. Because the fastest changes in fluxes occur in the early years of development, we evaluated the age dependence on a logarithmic scale (Figure 5). The coniferous stands consistently exhibited fluxes of greater magnitude than the hardwoods. Even though the absolute value of seasonal cumulative *ER* was greater in YHW than in YRP, it was at least partly caused by YHW being in a different stage of development. In the mature age group, the differences in *GEP* and *ER* cancelled out, and *NEE* was similar in MHW and MRP. Although PB does not fit in the developmental path of either hardwoods or conifers, it complements the age-dependent relationship. Because some unknown amount of C was lost from PB during the burn that created it, *ER* is likely suppressed at this site compared to what it would have been if this C had decomposed over multiple years like in YHW and YRP. It is obvious

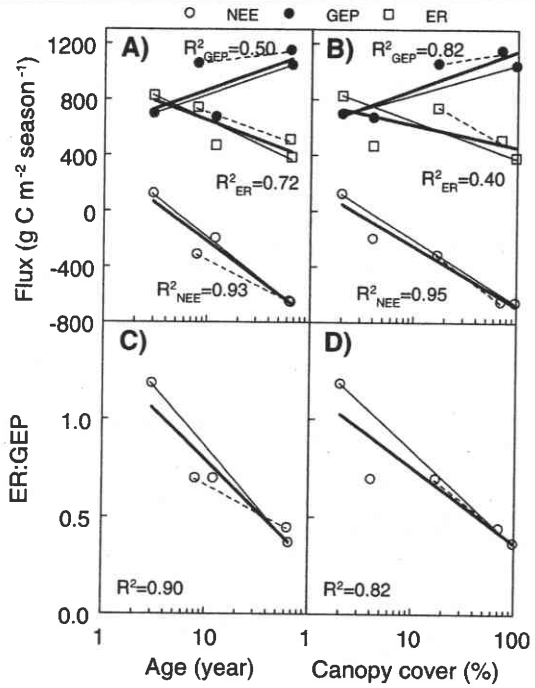

Figure 5. The relationship of cumulative C fluxes (**A**, **B**) and the *ER:GEP* ratio (**C**, **D**) with stand age (**A**, **C**) and percent canopy cover (**B**, **D**). Note that the abscissa is given in logarithmic scale. Hardwood stands (MHW, YHW) are connected with thin solid line, conifers (MRP, YRP) with *thin dashed line*. The coefficients of determination describe the age dependence of fluxes across all five stands, marked with *thick solid line*.

how the nature of stand-replacing disturbance could have dramatic effects on the trajectory of recovery. Whether the nature of disturbance affects the long-term C balance at the site is unclear and may depend on a number of additional factors.

Site differences in seasonal cumulative carbon fluxes correlated with differences in stand age and canopy cover (Figure 5a, b). Differences in *NEE* correlated equally well with either of these parameters, whereas those in *GEP* were better explained by canopy cover and those in *ER* by stand age. The observed patterns with age were similar to those reported for a chronosequence of Scots pine stands in Finland (Kolari and others 2004), which covered an age range comparable to current study. The correlation between *GEP* and canopy cover was to be expected because photosynthetic capacity depends directly on assimilating leaf area (see "Methods" for discussion on uncertainties about *LAI* estimates). The age dependence of *ER* encompasses simultaneous increase in autotrophic and decrease in heterotrophic respiration, as implied by the distribution of C in different pools (Table 1). The rapid increase in *ER* in YHW and YRP in June

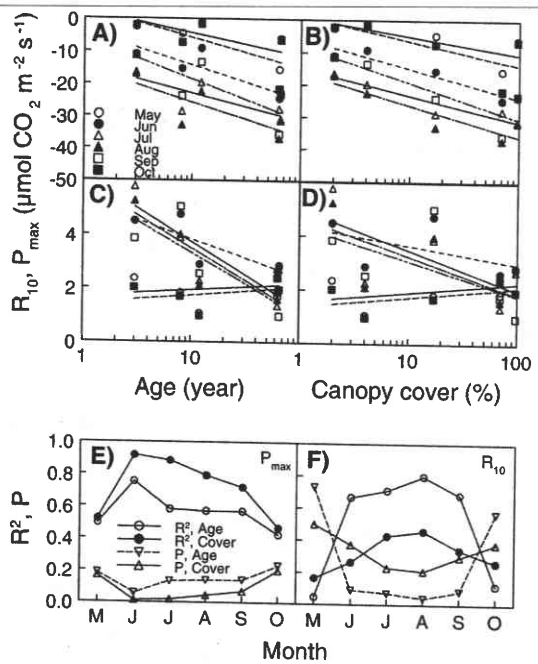

Figure 6. The relationship of P_{max} (**A**, **B**) and R_{10} (**C**, **D**) from Eq. 1 with stand age (**A**, **C**) and percent canopy cover (**B**, **D**) during different months of the study period. The coefficients of determination (R^2) and level of significance (P) of shown regressions are given as a function of time on two bottom panels, P_{max} (**E**) and R_{10} (**F**).

can be attributed to faster soil warming and the ready availability of substrate for *ER*. The increase in *ER* continued in July in YHW, but leveled off in YRP, even though stand differences in T_{S10} were minimal (<1.8°C). The rate of soil warming in spring correlated with canopy cover, which has a buffering effect on energy fluxes. The number of frost-free days (Ta_{min} > 0°C) and days with daily mean T_{S10} above 10°C were very similar in the young stands (only 2 days different in PB and YRP, and 10 days in YHW), whereas in the mature stands the difference was about a month (35 days in MHW, 28 days in MRP). In Ohio (41°33′N, 83°50′W) we found that T_{S10} equal to 10°C marks the threshold between plant dormancy and active growth (DeForest and others 2006). Depending on whether biological activity was constrained by soil temperature or the occurrence of night frosts, *ER* normalized for the number of favorable days would have stronger or weaker gradient with age. But regardless of the basis of expression, young stands consistently exhibited greater respiratory potential than mature stands. However, there may be a ramp-up period during the very first years after disturbance, before peak *ER* is reached (Humphreys and others 2005).

To evaluate the relative effects of environmental and physiological parameters on C fluxes, we analyzed the seasonal dynamics and age dependence of normalized gas exchange parameters, P_{max} and R_{10}. The age-dependent differences in P_{max} were significant and remained similar throughout the study period (Figure 6a, b), because of the similar seasonal dynamics of *GEP* in different stands (Figure 3b). The age-dependence of R_{10}, in contrast, exhibited distinct seasonality. The differences between stands were greatest in mid-season and smallest in spring and fall, and were caused by greater seasonal changes of R_{10} in the young than in the mature stands (Figure 6c, d). The significance of the age-dependence of P_{max} was also lower during May and October than mid-season, but less so than of R_{10} (Figure 6e, f). Overall, site differences in P_{max} correlated well with percent canopy cover, and differences in R_{10} with those in stand age (Figure 6), exhibiting similar trends as GEP and ER, respectively. Thus, the site differences in *ER* were driven primarily by more pronounced seasonal dynamics in the young than the mature stands (Figure 3c), and the compound effect of site differences in T_{S10} (dominant in spring), and R_{10} (dominant in summer).

The recovery of *GEP* after stand-replacing disturbance was faster than that of *ER* (Figure 3). The observation of rapid recovery generally supports the findings of earlier studies, although the nature of the disturbance and climatic conditions at any given site significantly affects whether and how much *ER* responds to the disturbance (Amiro 2001; Anthoni and others 2002; Law and others 2003; Kolari and others 2004; Humphreys and others 2005). In general, recent studies suggest that carbon fluxes recover rapidly after harvesting. For example, Amiro (2001) found that the greatest changes in post-disturbance recovery in boreal forests occurred in the first 10 years, although the C sink strength of a forest may continue to increase for 20 or even 30 years after a stand-replacing fire (Litvak and others 2003). Law and others (2001) concluded that it may take 10–20 years after harvest for ponderosa pine stands to become C sinks and 50–100 years to replace all C lost in a stand-replacing disturbance. Hicke and others (2003) also found, using remotely sensed normalized difference vegetation index (NDVI), that the average post-fire recovery period for net primary production in North American boreal forests was approximately 9 years. Barring large and divergent winter fluxes, the young stands measured in this study may also become C sinks within 10–15 years of

clearcutting, possibly sooner with burning (Figure 5). To assess the contribution of these regenerating forests to the regional C budget, we need to mechanistically understand the regulation of developmental changes in C exchange, the contribution of different component fluxes to *ER* and their dynamics after a stand-replacing disturbance.

The age-related differences in fluxes as well as gas exchange parameters among the five stands have implications for modeling landscape-level C exchange. However, the logarithmic relationships of C fluxes with stand age are likely to change in old-growth forests. Typically, the productivity of temperate and boreal forests peaks at the age of 50–70 years (Gower and others 1996; Pregitzer and Euskirchen 2004) and begins to decline thereafter because of various structural, physiological and environmental limitations (Ryan and others 1997), leading to a concomitant increase in respiration. Thus, the reported age-dependent relationships characterize the early part of forest development and should not be extrapolated beyond the covered age range. Yet, the majority of forests in the Great Lakes region are actively managed, second-growth stands less than 100 years old, and equilibrium old-growth stands are very rare.

Regulatory Mechanisms

Increased *ER* after a stand-replacing disturbance has been observed in some ecosystems (Kolari and others 2004; Kowalski and others 2004) but not in others (Amiro 2001; Law and others 2001; Litvak and others 2003; Kowalski and others 2004). Whether or not *ER* increases, seems to depend primarily on substrate availability. For example, harvesting was found to stimulate *ER* when logging residue was available as the substrate for heterotrophic respiration (Kolari and others 2004; Kowalski and others 2004) or when root activity was maintained even after harvest (Amiro 2001; Kowalski and others 2004). When *CWD* and litter were removed during a burn, however, *ER* decreased (Amiro 2001; Litvak and others 2003). Additional factors, such as changes in soil and air temperature and moisture may also affect *ER*, but can influence *ER* only when sufficient substrate is available. In this study, the only burned stand, PB, showed lower *ER* than the two harvested young stands (Figure 3c), even when considering their age difference. It supports the view that *CWD* may contribute significantly to *ER*, although we lack a quantitative assessment of the amount of carbon lost in the burn. Although at this stage we cannot attribute stand differences conclusively to either remaining root activity, aboveground plant activity, accelerated litter or *CWD* decomposition, the different management practices are likely to affect the rate and duration of ecosystem C loss.

It is clear that the post-disturbance increase in *ER* must originate from heterotrophic decomposition and could be caused by increased dead organic matter input, increased T_{S10} through increased radiative input and/or increased aeration of the top soil layers (Amiro 2001; Sun and others 2004). More negative *NEE* in the mature than in the young stands may also be associated with a shift in the balance between autotrophic (R_A) and heterotrophic (R_H) respiration (Anthoni and others 2002; Litvak and others 2003; Bolstad and others 2004). Changes in R_A may act through disturbance effects on root activity, mycorrhizal associations and soil properties. Studies that have partitioned *ER* to R_A and R_H have indeed found that R_H usually decreases with stand age (or, in some cases, remains constant), whereas R_A increases (Law and others 2001, 2003; Sun and others 2004). Given the different C pool sizes and turnover rates, it is R_H that determines a forest's ability to retain C in the long term.

In this study, the between-site differences in *NEE* resulted from the combined influences of both *GEP* and *ER*. The decreases of *ER* and *ER:GEP* ratio with stand age ($R^2 = 0.72$; Figures 3, 5) imply a shift in the balance between R_A and R_H, consistent with observed differences in *CWD*. However, the seasonal changes in the age-dependence of R_{10} and the uniformity of those of P_{max} (Figure 6) imply that the temporal window when age effects can manifest is longer for *GEP* than for *ER*. Thus, identifying the mechanistic connections may be difficult because several age-related parameters (for example, biomass, canopy cover, microclimate, and post-disturbance change in substrate type and availability for *ER*) are confounding or auto-correlated.

Summary

1 The age-dependent relationships of time-integrated C fluxes differed little among forests with different species composition.
2 The age-dependent differences in the assimilatory capacity (P_{max}) were consistent throughout the study period, whereas those in the respiratory capacity (R_{10}) lasted from June to September, and were not significant in May and October.
3 The seasonal dynamics of the *ER:GEP* ratio implied that *ER* was coupled to C supply from *GEP*

during most of the study period, but in spring and fall *ER* became more dependent on *CWD* and litter, particularly in the young, recently disturbed stands.

4 The between-site differences in seasonal *NEE* resulted from multiple sources of variability: assimilatory capacity (which depends on assimilating leaf area), *ER* (depends on substrate availability) and the duration of the growing season (depends on leaf habit in case of *GEP* and on temperature in case of *ER*).

ACKNOWLEDGMENTS

This study was supported by the National Science Foundation (DEB-0129405), Northern and Southern Global Change Programs of the USDA Forest Service, University of Toledo and US–China Carbon Consortium. We gratefully acknowledge the Washburn Ranger District for permission to carry out the study on their land and the staff at University of Wisconsin Agricultural Research Station in Ashland for logistical support. Sincere thanks to David Billesbach for advice regarding data processing protocols. Jared DeForest offered constructive comments on the earlier versions of the manuscript and Lise Waring edited the language. Soung-Ryoul Ryu provided soil C and N data, John Rademacher, Dan Wozniczka and Leif Williams assisted with field data collection and site maintenance.

REFERENCES

Amiro BD. 2001. Paired-tower measurements of carbon and energy fluxes following disturbance in the boreal forest. Global Change Biol 7:253–68.

Anthoni PM, Unsworth MH, Law BE, Irvine J, Baldocchi D, Van Tuyl S, Moore D. 2002. Seasonal differences in carbon and water vapor exchange in young and old-growth ponderosa pine ecosystems. Agric For Meteorol 111:203–22.

Bolstad PV, Davis KJ, Martin J, Cook BD, Wang W. 2004. Component and whole-system respiration fluxes in northern deciduous forests. Tree Physiol 24:493–504.

Bresee MK, LeMoine J, Mather SV, Crow TR, Brosofske K, Chen J. 2004. Detecting landscape dynamics in Chequamegon National Forest in northern Wisconsin, from 1972 to 2001, using Landsat imagery. Landscape Ecol 19:291–309.

Brosofske KD, Chen J, Crow TR. 2001. Understory vegetation and site factors: implications for a managed Wisconsin landscape. For Ecol Manage 146:75–87.

Burba G, Anderson DJ, Xu L, McDermitt DK. 2006. Correcting apparent off-season CO_2 uptake due o surface heating of an open path gas analyzer: progress report of an ongoing study. http://www.ams.confex.com/ams/pdfpapers/109731.pdf.

Chen JQ, Saunders SC, Crow TR, Naiman RJ, Brosofske KD, Mroz GD, Brookshire BL, Franklin JF. 1999. Microclimate in forest ecosystem and landscape ecology–variations in local climate can be used to monitor and compare the effects of different management regimes. BioSci 49:288–97.

Chen J, Paw U KT, Ustin SL, Suchanek TH, Bond BJ, Brosofske KD, Falk M. 2004. Net ecosystem exchanges of carbon, water, and energy in young and old-growth Douglas-fir forests. Ecosystems 7:534–44.

Cook BD, Davis KJ, Wang W, Desai A, Berger BW, Teclaw RM, Martin JG, Bolstad P, Bakwin PS, Yi C, Heilman WE. 2004. Carbon exchange and venting anomalies in an upland deciduous forest in northern Wisconsin, USA. Agric For Meteorol 126:271–95.

Davis KJ, Bakwin PS, Yi C, Berger BW, Zhao C, Teclaw RM, Isebrands JG. 2003. The annual cycles of CO_2 and H_2O exchange over a northern mixed forest as observed from a very tall tower. Global Change Biol 9:1278–93.

DeForest JL, Noormets A, McNulty SG, Sun G, Tenney G, Chen J. 2006. Phenophases alter the soil respiration-temperature relationship in an oak-dominated forest. Int J Biomet 51:135–144.

Desai AR, Noormets A, Bolstad PV, Chen J, Cook BD, Davis KJ, Euskirchen ES, Gough C, Martin JM, Ricciuto DM, Schmid HP, Tang J, Wang W. 2007. Influence of vegetation type, stand age and climate on carbon dioxide fluxes across the Upper Midwest, USA: implications for regional scaling of carbon flux. Agric For Meteorol, in press.

Falge E, Baldocchi D, Olson R, Anthoni P, Aubinet M, Bernhofer C, Burba G, Ceulemans R, Clement R, Dolman H, Granier A, Gross P, Grünwald T, Hollinger D, Jensen N-O, Katul G, Keronen P, Kowalski A, Lai CT, Law BE, Meyers T, Moncrieff J, Moors E, Munger JW, Pilegaard K, Rannik ü, Rebmann C, Suyker A, Tenhunen J, Tu K, Verma S, Vesala T, Wilson K, Wofsy S. 2001. Gap filling strategies for defensible annual sums of net ecosystem exchange. Agric For Meteorol 107:43–69.

Falge E, Baldocchi DD, Tenhunen J, Aubinet M, Bakwin PS, Berbigier P, Bernhofer C, Burba G, Clement R, Davis KJ, Elbers JA, Goldstein AH, Grelle A, Granier A, Guddmundsson J, Hollinger D, Kowalski AS, Katul G, Law BE, Malhi Y, Meyers T, Monson RK, Munger JW, Oechel W, Paw U KT, Pilegaard K, Rannik ü, Rebmann C, Suyker A, Valentini R, Wilson K, Wofsy S. 2002. Seasonality of ecosystem respiration and gross primary production as derived from FLUXNET measurements. Agric For Meteorol 113:53–74.

Goulden ML, Munger JW, Fan SM, Daube BC, Wofsy SC. 1996. Measurements of carbon sequestration by long-term eddy covariance: methods and critical evaluation of accuracy. Global Change Biol 2:169–82.

Gower ST, McMurtrie RE, Murty D. 1996. Aboveground net primary production decline with stand age: potential causes. Trends Ecol Evol 11:378–82.

Harmon ME, Franklin JF, Swanson FJ, Sollins P, Gregory SV, Lattin JD, Anderson NH, Cline SP, Aumen NG, Sedell JR, Lienkaemper GW, Cromack K, Cummins KW. 1986. Ecology of coarse woody debris in temperate ecosystems. Adv Ecol Res 15:133–302.

Hicke JA, Asner GP, Kasischke ES, French NHF, Randerson JT, Collatz GJ, Stocks BJ, Tucker CJ, Los SO, Field CB. 2003. Postfire response of North American boreal forest net primary productivity analyzed with satellite observations. Global Change Biol 9:1145–57.

Högberg P, Nordgren A, Buchmann N, Taylor AFS, Ekblad A, Högberg MN, Nyberg G, Ottosson-Lofvenius M, Read DJ. 2001. Large-scale forest girdling shows that current photosynthesis drives soil respiration. Nature 411:789–92.

Houghton JT, Ding Y, Griggs DJ, Noguer M, Van der Linden PJ, Da X, Maskell K, Johnson CA. 2001. Climate change 2001: the scientific basics. Cambridge: Cambridge University Press, p 944.

Howard EA, Gower ST, Foley JT, Kucharik CJ. 2004. Effects of logging on carbon dynamics of a jack pine forest in Saskatchewan, Canada. Global Change Biol 10:1267–84.

Humphreys ER, Black TA, Morgenstern K, Li Z, Nesic Z. 2005. Net ecosystem production of a Douglas-fir stand for 3 years following clearcut harvesting. Global Change Biol 11:450–64.

Janssens IA, Lankreijer H, Matteucci G, Kowalski AS, Buchmann N, Epron D, Pilegaard K, Kutsch W, Longdoz B, Grünwald T, Montagnani L, Dore S, Rebmann C, Moors EJ, Grelle A, Rannik ü, Morgenstern K, Oltchev S, Clement R, Guðmundsson J, Minerbi S, Berbigier P, Ibrom A, Moncrieff J, Aubinet M, Bernhofer C, Jensen NO, Vesala T, Granier A, Schulze E-D, Lindroth A, Dolman AJ, Jarvis PG, Ceulemans R, Valentini R. 2001. Productivity overshadows temperature in determining soil and ecosystem respiration across European forests. Global Change Biol 7:269–78.

Kolari P, Pumpanen J, Rannik ü, Ilvesniemi H, Hari P, Berninger F. 2004. Carbon balance of different aged Scots pine forests in Southern Finland. Global Change Biol 10:1106–19.

Kowalski AS, Loustau D, Berbigier P, Manca G, Tedeschi V, Borghetti M, Valentini R, Kolari P, Berninger F, Rannik ü, Hari P, Rayment M, Mencuccini M, Moncrieff J, Grace J. 2004. Paired comparisons of carbon exchange between undisturbed and regenerating stands in four managed forests in Europe. Global Change Biol 10:1707–23.

Law BE, Thornton PE, Irvine J, Anthoni PM, Van Tuyl S. 2001. Carbon storage and fluxes in ponderosa pine forests at different developmental stages. Global Change Biol 7:755–77.

Law BE, Falge E, Guc L, Baldocchi DD, Bakwin PS, Berbigier P, Davis KJ, Dolman AJ, Falk M, Fuentes JD, Goldstein AH, Granier A, Grelle A, Hollinger D, Janssens IA, Jarvis PG, Jensen N-O, Katul G, Malhi Y, Matteucci G, Meyers T, Monson RK, Munger JW, Oechel W, Olson R, Pilegaard K, Paw U KT, Thorgeirsson H, Valentini R, Verma S, Vesala T, Wilson K, Wofsy S. 2002. Environmental controls over carbon dioxide and water vapor exchange of terrestrial vegetation. Agric For Meteorol 113:97–120.

Law BE, Sun OJ, Campbell J, Van Tuyl S, Thornton PE. 2003. Changes in carbon storage and fluxes in a chronosequence of ponderosa pine. Global Change Biol 9:510–24.

Lee X, Massman WJ, Law BE. 2004. Handbook in micrometeorology. A guide for surface flux measurement and analysis. vol. 29. Dordrecht: Kluwer, p 250.

Leuning R. 2004. Measurements of trace gas fluxes in the atmosphere using eddy covariance: WPL corrections revisited. In: Lee X, Massman WJ, Law BE, Lee X, Massman WJ, Law BEs, Eds. Handbook of micrometeorology. A guide to surface flux measurement and analysis. Boston: Kluwer. pp 119–32.

Litvak M, Miller S, Wofsy SC, Goulden M. 2003. Effect of stand age on whole ecosystem CO_2 exchange in the Canadian boreal forest. J Geophys Res–Atmos 108:art. no. 8225.

Noormets A, Desai A, Cook BD, Ricciuto DM, Euskirchen ES, Davis K, Bolstad P, Schmid HP, Vogel CS, Carey EV, Su H-B, Chen J. 2007. Moisture sensitivity of ecosystem respiration: comparison of 14 forest ecosystems in the Upper Great Lakes Region, USA. Agric For Meteorol, in press.

Paw U KT, Baldocchi DD, Meyers T, Wilson KB. 2000. Correction of eddy-covariance measurements incorporating both advective effects and density fluxes. Boundary-Layer Meteorol 97:487–511.

Paw U KT, Falk M, Suchanek TH, Ustin SL, Chen J, Park Y-S, Winner WE, Thomas SC, Hsiao TC, Shaw RH, King TS, Pyles RD, Schroeder M, Matista AA. 2004. CO_2, H_2O, and energy fluxes of an old-growth forest. Ecosystems 7:513–24.

Potter C, Tan PN, Steinbach M, Klooster S, Kumar V, Myneni R, Genovese V. 2003. Major disturbance events in terrestrial ecosystems detected using global satellite data sets. Global Change Biol 9:1005–21.

Pregitzer KS, Euskirchen ES. 2004. Carbon cycling and storage in world forests: biome patterns related to forest age. Global Change Biol 10:2052–77.

Richardson AD, Hollinger DY, Burba GG, Davis KJ, Flanagan LB, Katul GG, Munger JW, Ricciuto DM, Stoy PC, Suyker AE, Verma SB, Wofsy SC. 2006. A multi-site analysis of random error in tower-based measurements of carbon and energy fluxes. Agric For Meteorol 136:1–18.

Ryan MG, Binkley D, Fownes JH. 1997. Age-related decline in forest productivity: pattern and process. Adv Ecol Res 27:213–62.

Schmid HP, Su H-B, Vogel CS, Curtis PS. 2003. Ecosystem-atmosphere exchange of carbon dioxide over a mixed hardwood forest in northern lower Michigan. J Geophys Res 108, NO. D14, 4417, doi:10.1029/2002JD003011:6.1-6.19.

Schotanus P, Nieuwstadt FTM, de Bruin HAR. 1983. Temperature measurement with a sonic anemometer and its application to heat and moisture fluxes. Boundary-Layer Meteorol 26:81–93.

Sun OJ, Campbell J, Law BE, Wolf V. 2004. Dynamics of carbon stocks in soils and detritus across chronosequences of different forest types in the Pacific Northwest, USA. Global Change Biol 10:1470–81.

Turner DP, Guzy M, Lefsky MA, Van Tuyl S, Sun O, Daly C, Law BE. 2003. Effects of land use and fine-scale environmental heterogeneity on net ecosystem production over a temperate coniferous forest landscape. Tellus B 55:657–68.

Webb EK, Pearman GI, Leuning R. 1980. Correction of flux measurements for density effects due to heat and water vapor transfer. Quart J R Meteorol Soc 106:85–106.

Wilczak JM, Oncley SP, Stage SA. 2001. Sonic anemometer tilt correction algorithms. Boundary-Layer Meteorol 99:127–50.